

Studies on the Mechanism of Interaction of a Bioresponsive Endosomolytic Polyamidoamine with Interfaces. 1. Micelles as Model Surfaces

Peter C. Griffiths,^{†,*} Zeena Khayat,^{†,‡} Stephanie Tse,[†] Richard K. Heenan,[§]
Stephen M. King,[§] and Ruth Duncan[‡]

School of Chemistry, Cardiff University, Main Building, Park Place, Cardiff CF10 3AT, U.K., Centre for Polymer Therapeutics, Welsh School of Pharmacy, Redwood Building, King Edward's VII Avenue, Cardiff CF10 3XF, U.K., and ISIS Facility, Rutherford Appleton Laboratory, Chilton, Didcot OX11 0QX, U.K.

Received September 28, 2006; Revised Manuscript Received December 7, 2006

Polymers are appealing as pH-responsive elements of multicomponent systems designed to promote cytosolic delivery of macromolecular drugs (including proteins and genes), but so far the delivery efficiency achieved has been relatively modest. Therefore, the aim of this study was to apply several physicochemical techniques that are well established in the colloid field (surface tension measurements, small-angle neutron scattering (SANS), and electron paramagnetic resonance (EPR)) to probe the mechanism of endosomolytic polymer–surface interaction over the pH range 7.4 to 5.5 using the poly(amidoamine) (PAA) ISA23·HCl and a series of “model” micelle surfaces. These micellar models were chosen to represent increasing complexity from simple, single surfactant sodium dodecylsulfate (SDS) micelles, surfactant mixtures containing bulky malono-bis-N-methylglucamide headgroups, or highly extended ethylene oxide headgroups. Spherical micelles composed of 1-palmitoyl-2-hydroxy-sn-glycero-3-phosphocholine (lyso-PC) were also used. Changes in the onset of micellization, micelle surface fluidity, and in selected cases, the overall micelle shape and size were all quantified as a function of pH in the presence and absence of ISA23·HCl. This amphoteric PAA is negatively charged at pH 7.4 and becomes gradually more protonated on exposure to lower pH values representative of the endosomal–lysosomal pathway. As expected, the strength of polymer interaction with anionic micelles increased with a decrease in pH, while for cationic micelles the opposite was observed. Addition of bulky, nonionic surfactant headgroups led to weaker interactions. The observations from surface tension and SANS studies showed a complex pattern of interaction with both an electrostatic and hydrophobic component. Using EPR it was confirmed that ISA23·HCl perturbed the micelle palisade layer leading to a decrease in fluidity of the interface with a lower degree of headgroup hydration, and a significant change in micelle morphology. Surprisingly, there was no interaction between ISA23·HCl and globular micelles formed from lyso-PC (a more biologically relevant model), and this suggests that the PAA structure could be better optimized to promote rapid interaction with endosomal membranes at the physiologically relevant pH 6.5.

Introduction

Despite increased understanding of the molecular basis of many diseases, the challenge of identification of safe and effective delivery systems able to localize macromolecular drugs (including peptide, protein, gene, and polymer therapeutics) into the cytosol of the target diseased cells remains. Once there, such vectors must also promote efficient delivery to the correct intracellular compartment. Retroviral and adenoviral vectors are currently favored as tools for gene therapy,¹ as they promote highly efficient gene delivery; however, there are still concerns, as viral vectors have a mixed safety record.^{2–4} This has led to a concerted effort to design nonviral delivery vectors using endosomolytic polymers that can efficiently promote cytosolic access.^{5–7}

In this context, we have been designing linear poly(amidoamine)s (PAAs) as pH-responsive endosomolytic polymers for gene and toxin delivery.^{8–11} Specific PAA structures (ISA23·

HCl and ISA4·HCl) have shown considerable promise.⁹ They have relatively low toxicity compared to other cationic vectors (>100 fold less toxic than poly(ethylene imine) PEI and poly-L-lysine PLL), and the ability (ISA23·HCl) to escape reticuloendothelial cell clearance, allowing tumor targeting by enhanced permeability and retention (EPR) effect targeting.⁹ However, experiments studying the cytosolic delivery of genes¹⁰ and nonpermeant protein toxins¹¹ showed that efficiency of delivery was still not sufficiently high to warrant further development toward *in vivo*/clinical applications.

To guide the development of more effective PAA chemistries better able to promote rapid (within <10 min), transient, and highly efficient endosomal permeabilization at pH 6.5, we have begun to define more carefully the physicochemical properties of ISA23·HCl in relation to the desired bioactivity using techniques that are more usually used in the colloid field.^{12–14} First studies used SANS and pulsed-gradient spin-echo NMR, and they showed that ISA23·HCl adopts a rather compact random coiled structure at pH 7.4 with a radius of gyration (R_g) of ~2 nm. As pH was lowered, the polymer coil gradually expanded to a maximum of ~8 nm at pH = 3 before coil collapse. The main aim of this study was to examine for the

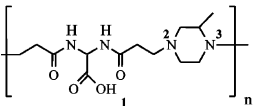
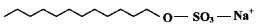
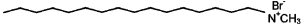
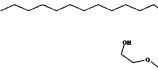
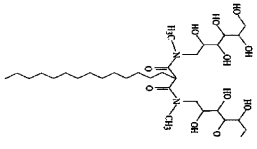
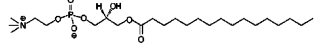
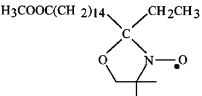
* Corresponding author. E-mail: GriffithsPC@Cardiff.ac.uk; phone: +44(0)29-20875858; fax: +44(0)29-20874030.

[†] Cardiff University.

[‡] Welsh School of Pharmacy.

[§] Rutherford Appleton Laboratory.

Table 1. Surfactants and Other Species Used in This Study

compound	code	structure
poly(amidoamine)	ISA23.HCl	
sodium dodecylsulfate	SDS	
cetyl trimethyl ammonium bromide	CTAB	
tetra(ethylene oxide) dodecyl ether	C ₁₂ E ₄	
<i>n</i> -dodecyl malono-bis- <i>N</i> -methylglucamide	C ₁₂ BNMG	
1-palmitoyl-2-hydroxy- <i>sn</i> -glycero-3-phosphocholine	lyso-PC	
16-doxyl stearic acid methyl ester	16-DSE	

first time the effect of pH on the interaction of ISA23·HCl and a series of “model” surfaces. A library of micelles (Table 1) was used, chosen to represent increasing complexity (single surfactant SDS micelles, surfactant mixtures containing bulky or highly extended headgroups using a systematic change of composition) and more biologically relevant lyso-PC micelles. Surface tension measurements and small-angle neutron scattering (SANS) studies were undertaken to investigate the pH-dependent interaction of ISA23·HCl with micelles of different composition, and the electron paramagnetic resonance (EPR) probe 16-doxyl stearic acid methyl ester (16-DSE) was used to study the effect of the polymer on micelle fluidity.

Materials and Methods

Materials. Sodium dodecylsulfate (SDS) (Aldrich) was purified by repeated recrystallization from ethanol until no impurities could be detected in the surface tension data (a minimum or “dip” around the critical micelle concentration (CMC)). Deuterated SDS (d-SDS) (Aldrich), cetyltrimethylammonium bromide (CTAB) (Aldrich, analytical grade), the spin-probe 16-DSE (Fluka, analytical grade), D₂O (Aldrich), tetra(ethylene oxide) dodecyl ether (C₁₂E₄) (Aldrich), and 1-palmitoyl-2-hydroxy-*sn*-glycero-3-phosphocholine (lyso-PC) (Avanti Polar Lipids, purity >99%) were all used as received. The sugar based surfactant *n*-dodecyl malono-bis-*N*-methylglucamide (C₁₂BNMG) was a gift from Kodak Ltd. Before use, this surfactant was purified by HPLC using a C₁₈ reverse phase column with as mobile phase 80%/20% methanol (HPLC grade)/double distilled water. The monomers; 2,2-bis-(acrylamido)acetic acid (BAC) was a kind gift from P. Ferruti (University of Milan) and was synthesized as previously described.¹⁵ 2,2-Methylpiperazine (2-MePip) was purchased from Fluka and was recrystallized from *n*-heptane and its purity determined titrimetrically before use.

Synthesis of ISA23·HCl. ISA23·HCl was synthesized by polyaddition of BAC and 2,2-MePip as previously described.⁹ Briefly, BAC

Table 2. Composition of Micelles Used To Prepare the Model Surfaces for This Work

model	SDS	C12E4	C12BNMG	CTAB	lyso-PC
1	1.00	-	-	-	-
2	-	1.00	-	-	-
3	-	-	1.00	-	-
4	-	-	-	1.00	-
5	-	-	-	-	1.00
6	0.90	0.10	-	-	-
7	0.75	0.25	-	-	-
8	0.50	0.50	-	-	-
9	0.50	-	0.50	-	-
10	-	-	0.50	0.50	-

^a Solution compositions expressed in terms of the surfactant mole fraction (α) according to $\alpha_{\text{interacting}} = [\text{surfactant}]_{\text{ionic}} / [\text{surfactant}]_{\text{ionic}} + [\text{surfactant}]_{\text{nonionic}}$ where the square brackets denote concentration and ionic refers to SDS, CTAB, or lyso-PC, and nonionic refers to C₁₂E₄ or C₁₂BNMG.

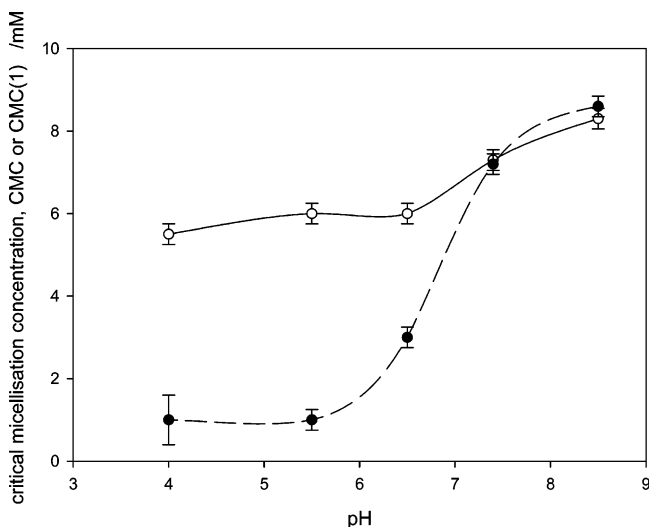


Figure 1. Critical micelle concentrations of aqueous solutions of sodium dodecyl sulfate (SDS) (at 37 °C) in the absence (open symbols) and presence (filled symbols) of ISA23·HCl (0.2 wt %) as a function of pH.

(1 g; 5 mmol) and LiOH·H₂O (0.212 g; 5 mmol) were dissolved in double distilled water (to give a BAC concentration of 3 M; 1.67 mL). The mixture was stirred for 10 min, 2-MP (0.511 g; 5 mmol) was added, and after further stirring for 3 days at 25 °C under a nitrogen atmosphere in the dark, the reaction was stopped by adding water. HCl was then added to the mixture, until the pH reached 3–4. The reaction mixture was then filtered using a stirred ultrafiltration cell (model 8200, Amicon, Bioseparation, Millipore), with membrane cut off 10 000 g/mol to purify the polymer. Product identity was confirmed by ¹H NMR. The polymer had a molecular weight M_w of 65 500 g/mol and an M_w/M_n of 2.1 (by gel permeation chromatography (GPC) using poly(vinylpyrrolidone) (PVP) standards). It should be noted that the pK_a values for ISA23·HCl are $pK_{a1} = 2.1$; $pK_{b2} = 7.5$; $pK_{b3} = 3.3$ (Table 1).

Measurement of Surface Tension Using Model Micelles. The surface tension measurements were made using either a Du Nöuy ring surface tension balance incorporating a CI Electronics zero displacement microbalance with a platinum ring of 4 cm circumference or a maximum bubble pressure tensiometer (SITA Online t60) with bubble lifetime of 10 s as previously described.^{16–17} Both instruments were calibrated using water/ethanol mixtures. In all cases, measurements were made at 37 °C ± 0.5. All glassware was thoroughly cleaned with Decon90 and rinsed with copious quantities of pure water. First, stock surfactant solutions were prepared by dissolving the appropriate mass of surfactant

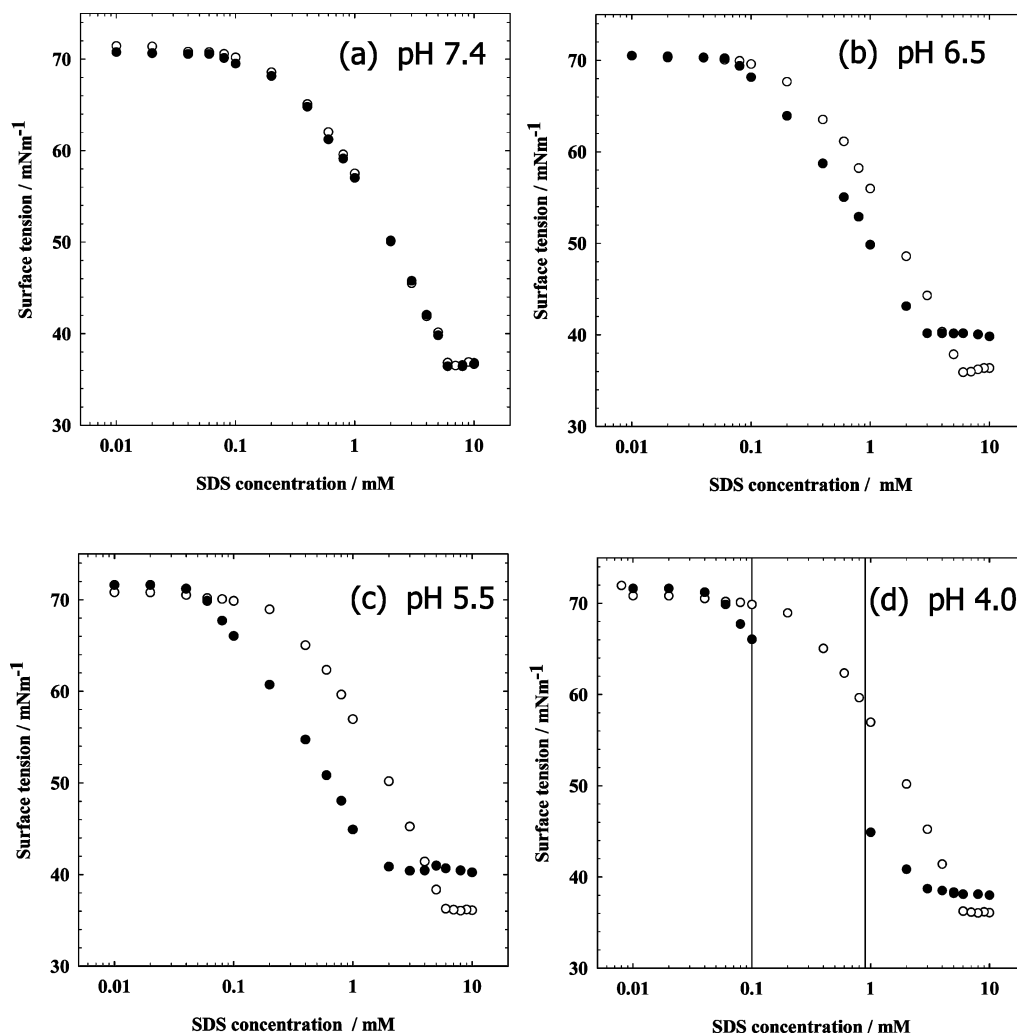


Figure 2. The effect of pH on the micellization of sodium dodecyl sulfate (SDS) in the absence (open circles) and presence (filled circles) of ISA23-HCl (0.2 wt %).

in distilled water to produce a total surfactant concentration of 25 mM and the ratios shown in Table 2. The stock solution of ISA23-HCl (0.4 w/v% in double distilled water) was prepared, and the final pH was measured and adjusted accordingly to the desired value for each experiment using HCl or NaOH. Then, the surface tension of this surfactant solution was measured in the presence or the absence of ISA23-HCl as a function of pH as follows. Serial dilutions were prepared to obtain different surfactant concentrations, 3 mL of each was added to a glass vial, and the surface tension was measured using the maximum bubble pressure tensiometer (with a bubble lifetime of 10 s). For the samples containing a mixture of ISA23-HCl and surfactant, a 1.5 mL of surfactant and a 1.5 mL of ISA23-HCl (final polymer concentration of 0.2 w/v%) were added to a glass vial and left to equilibrate for 10 min, and the surface tension was measured as above. Measurements were made at pH 4–8. Initial studies demonstrated excellent reproducibility between the Du Nöuy ring and maximum bubble pressure methods, and accordingly, the maximum bubble pressure tensiometer was predominantly used in order to minimize sample volumes.

Investigation of Polymer–Micelle Interaction Using Small-Angle Neutron Scattering. To study SDS micelle–ISA23-HCl interaction, stock solutions of SDS (50 mM) were prepared in D₂O, and the pH was adjusted to the required value (pH 7.4, 5.5, or 4). ISA23-HCl solutions were also prepared (concentration of 2 w/v%) at pH 7.4, 5.5, or 4. Prior to the SANS measurements, 1.5 mL of SDS and 1.5 mL ISA23-HCl solution were mixed. In the case of the lyso-PC micelles, a solution of lyso-PC (10 mM) was prepared at pH 5.5 or 7.4 and mixed with a solution of ISA23-HCl (2 w/v %) at pH 7.4 and 5.5.

All SANS measurements were performed on the LOQ diffractometer at the ISIS Spallation Neutron Source, Oxfordshire. The scattering data were normalized for the sample transmission and incident wavelength distribution, background corrected, and corrected for the linearity and efficiency of the detector response. LOQ is a fixed-geometry, time-of-flight (TOF) instrument and using wavelengths between 2 and 10 Å, spans a Q -range ~ 0.001 to 0.3 Å^{-1} . For the SANS samples, serial dilution was also used to generate the samples, but in this case, D₂O (Goss Scientific) was used in the place of pure water, and all experiments were conducted at 37 °C.

For globular micelles, the analytical procedure of Hayter and Penfold^{18–20} for quantifying micelle structure from SANS data was used. For a solution of interacting charged micelles, the intensity of scattered radiation, $I(Q)$, as a function of the wave-vector, Q , is given by;

$$I_{\text{surfactant}}(Q) = n[S(Q)\langle|F(Q)|^2\rangle + \langle|F(Q)|^2\rangle - \langle F(Q)\rangle\langle F(Q)\rangle] + B_{\text{inc}} \quad (1)$$

where $F(Q) = V_1(\rho_1 - \rho_2)F_0(QR_1) + V_2(\rho_2 - \rho_0)F_0(QR_2)$

The first term represents the scattering from the hydrocarbon core (subscript 1) and the second the polar shell (subscript 2). $V_i = 4/3\pi R_i^3$ and $F_0(QR) = \{3j_1(QR)\}/\{QR\}$ where j_1 is the first-order spherical Bessel function of the first kind. $S(Q)$ represents the spatial arrangement of the micelles in solution and n the micelle number density. Equation 1 invokes the “decoupling approximation”, i.e., there is no correlation between the position of the micelle and its orientation. ρ_1 is the neutron scattering length density of the micellar core (subscript 1), the polar

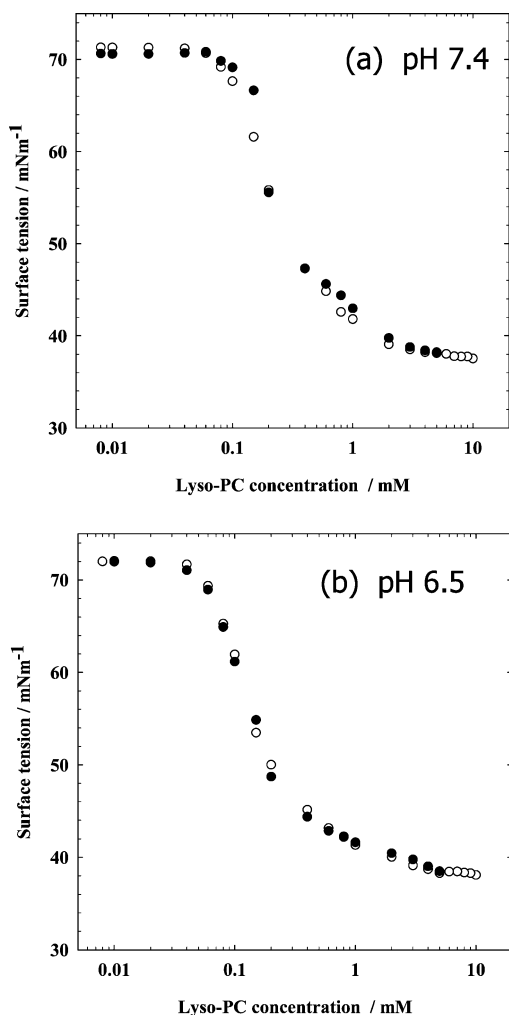


Figure 3. The effect of pH on the micellization of 1-palmitoyl-2-hydroxy-*sn*-glycero-3-phosphocholine (lyso-PC) in the absence (open circles) and presence (filled circles) of ISA23-HCl (0.2 wt %).

shell (subscript 2), and the solvent (subscript 0). These constants were combined into a single fittable parameter used to “scale” the model intensity to the absolute value. Postfitting, this scalar was recalculated using the parameters describing the micelle morphology/composition and the molar concentration of micelles to validate the fit. The calculated and observed values should lie within $\sim 10\%$.

The structure factor $S(Q)$ was calculated using the Hayter and Penfold model^{18–20} for spheres of a given micellar concentration, charge, and ionic strength, incorporating refinements for low volume fractions and a penetrating ionic background. This function was parametrized *via* a hard sphere radius and volume fraction, the surface charge on the micelle, and the Debye screening length.

Use of Electron Paramagnetic Resonance To Study Micelle Fluidity. EPR was used to study the effect of pH and ionic strength on the fluidity of SDS micelles. First, micelles were prepared by addition of 5 mL of SDS (25 mM in pure water) to glass vials containing predried spin-probe 16-DSE (0.04 mg/mL; the ratio of the SDS to spin probe was $\sim 500:1$), mixed, and allowed to equilibrate. The pH was adjusted by addition of HCl. Similarly, the polymer/surfactant series were prepared by adding SDS (50 mM, 2.5 mL) and ISA23-HCl (0.4 w/v%; 2.5 mL) to a glass vial containing predried spin-probe (16-DSE). To study the interaction between the lyso-PC micelle and ISA23-HCl, an analogous protocol was adopted. First as a control, a 5 mL solution of lyso-PC (10 mM) was added to predried 16-DSE (as above), and the pH was adjusted to the desired value by the addition of HCl or NaOH. In parallel, lyso-PC (20 mM) and ISA23-HCl (0.4 w/v%) were added to a separate glass vial containing dried spin-probe. Before EPR measurements, the pH of the solution was measured and then an aliquot

of the sample drawn into a capillary tube which was sealed and placed in quartz EPR tubes before taking measurements using a Bruker EMX at room temperature ($\sim 22^\circ\text{C}$) using a frequency of 9.29 ± 0.3 GHz. Each spectrum was recorded as the average of five scans.

The resultant spectra were transferred to a PC and the lineshapes fitted using LOWFIT^{21–23} to a Voigt approximation to separate the Gaussian and Lorentzian components of the spectral lines and to locate the resonance fields of the three EPR lines to a precision of a few mG. The separation A^+ of the low and center lines ($M_I = +1$ and $M_I = 0$) is directly related to the polarity index $H(25^\circ\text{C})$, defined as the molar ratio of OH groups in a given volume relative to water;

$$A^+ = 14.309 + 1.419 H(25^\circ\text{C}) \quad (2)$$

For simple surfactant solutions such as SDS, $H(25^\circ\text{C})$ corresponds directly to the volume fraction of water in the polar shell. For surfactants such as lyso-PC that possess an OH group as an integral part of its headgroup, $H(25^\circ\text{C})$ requires a straightforward volume correction.²⁴

Results

Surface Tension Measurements. The micellization of the anionic surfactant SDS was studied in the presence and absence of ISA23-HCl over the pH range $4 < \text{pH} < 9$ (Figures 1 and 2). The CMC of SDS alone decreased smoothly with decreasing pH (Figure 1; data derived from Figure 2), but this was as a result of the increasing ionic strength rather than the pH *per se*. At pH 8.5 the CMC was 8.2 ± 0.1 mM, and the surface area per SDS molecule was 0.5 ± 0.06 nm², as expected.²¹ It can be seen that under conditions where the amphoteric polymer bears a significant net negative charge, e.g., pH 7.4 (Figure 2a), addition of the polymer to the anionic surfactant caused no change in either surface tension or CMC indicating no interaction. However, as the pH was lowered, the polymer and anionic surfactant start to interact (Figures 2b,c). At pH 4.0 the polymer bears a net positive charge (Figure 2d), and this strong interaction led to phase separation, as delineated by the two vertical lines. Accordingly, any measurement of surface tension under these conditions would be meaningless and therefore is reported. A critical pH value ($\text{pH}^{\text{crit}}(\text{CMC})$) occurs when there is a difference between the CMC seen in the absence and the presence of the polymer (CMC_1), in this case approximately $\text{pH } 7.1 \pm 0.2$. The difference between the CMC and the CMC_1 increased as pH decreased, and at pH 5 the differences in free energy changes ($\Delta G = -RT \ln \text{CMC}$) involved in micellization corresponds to ~ 2 kJ mol^{−1}; this is the additional driving force to form the polymer–SDS complex.

Conversely, when the ISA23-HCl interaction with a cationic surfactant CTAB was studied at pH 7.4 (i.e., when the polymer bears the opposite charge to the surfactant), a strong interaction was observed, again leading to phase separation. With decreasing pH, the interaction became weaker, and ultimately, at pH 4, the polymer had little effect on the surface tension of the mixture, indicating that the interaction had been “turned off” (data not shown). In contrast, neither of the nonionic surfactants C₁₂BNMG and C₁₂E₄ alone showed any interaction with ISA23-HCl. Moreover, when the SDS micelle mixtures listed in Table 2 were studied, in all cases, introduction of the nonionic surfactant rendered the interaction, at any given pH, weaker than the interaction observed in the corresponding ISA23-HCl–SDS case.

All the data obtained for the surfactant mixtures can be compared qualitatively if the surfactant mole fraction is taken into account (see Table 2). At pH 4, in the case of the ISA23-HCl /SDS/C₁₂E₄ mixtures (for all $\alpha_{\text{interacting}}$ values) and for

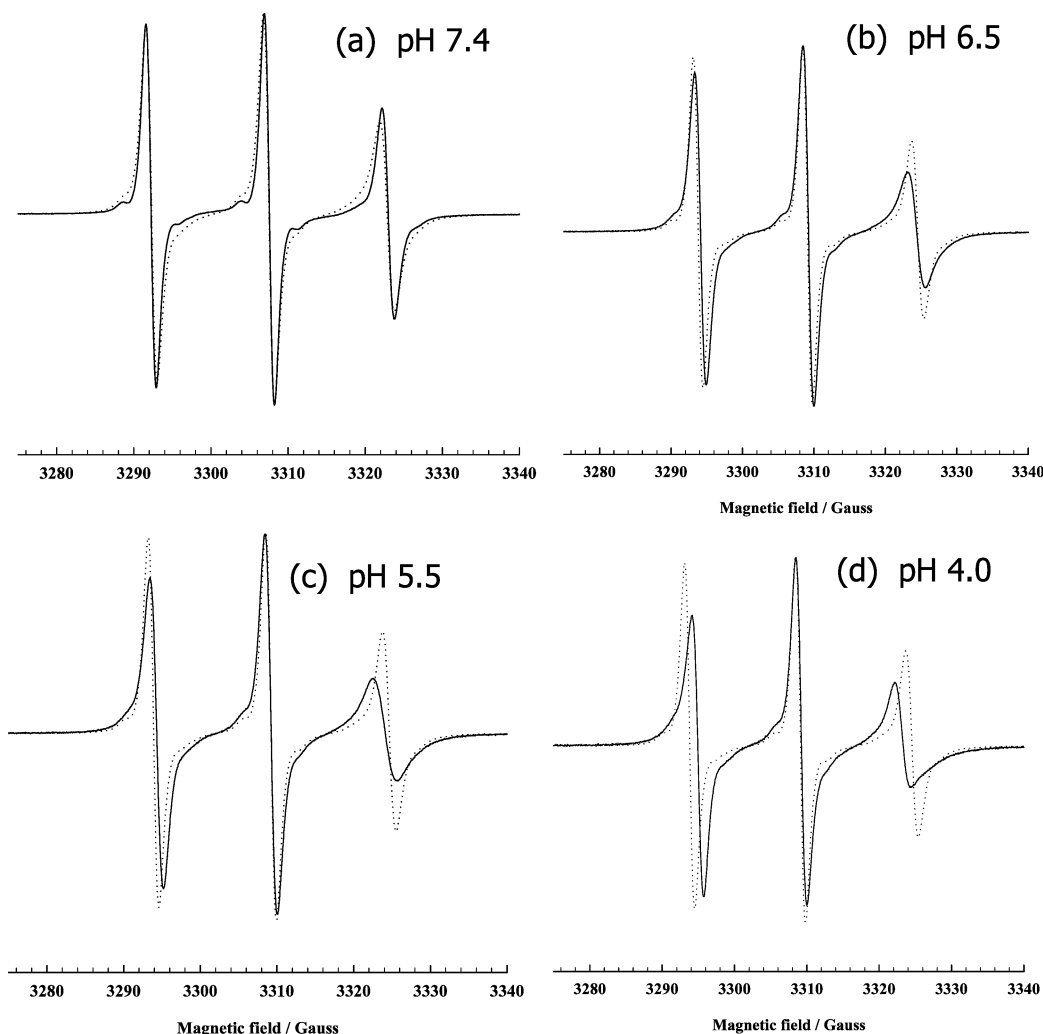


Figure 4. The effect of pH on the EPR spectrum of 16DSE solubilized in aqueous solutions of sodium dodecyl sulfate (SDS) in the absence (broken line) and presence (solid line) of ISA23-HCl (0.2 wt %).

ISA23-HCl /SDS/ C_{12} BNMG micelles at $\alpha_{\text{interacting}} = 0.5$, a strong interaction was seen. For the ISA23-HCl/SDS/ C_{12} E₄ mixture having an $\alpha_{\text{interacting}} = 0.9$, an interaction was observed at pH 5, but not at pH values > 6 . Using these mixtures having $\alpha_{\text{interacting}} = 0.75$ and 0.5 , no interaction was observed at all pH values > 5 . In contrast, addition of ISA23-HCl to the ISA23-HCl/CTAB/ C_{12} BNMG mixture having $\alpha_{\text{interacting}} = 0.5$, precipitation occurred at pHs > 7 , but no interaction was observed for pH values less than 4.

Surprisingly, when surface tension measurements were used to study ISA23-HCl interaction with small spherical micelles formed from lyso-PC, it was found that the surface tension behavior was unaltered following the addition of ISA23-HCl at pH 7.4 or pH 5.5 (Figure 3). The EPR spectroscopy experiments were only conducted using the single surfactant micelles (SDS, Figure 4 and lyso-PC, Figure 5) and pairwise spectral comparisons are shown at each pH. Small changes in peak intensity arising due to slight changes in instrument gain were removed by normalizing each spectrum to the maximum peak intensity in each spectrum. For SDS, at pH = 7.4 (Figure 4a) there was no *significant* difference in the EPR spectra obtained in the absence and presence of the polymer indicating no interaction between the SDS and ISA23-HCl. Addition of the polymer affects the bulk viscosity of the system, and therefore some reduction in the micelle mobility (tumbling) was to be expected.^{25–27} As the pH decreased, visible changes in line width and intensity were evident (Figures 4b,c). This was most striking

at pH 4.5 (Figure 4d). The decreasing intensity of the low field peak was particularly important, as this indicated that the motion of the spin-probe had become anisotropic and/or very slow.

From the EPR hyperfine coupling of the 16-DSE solubilized in the ISA23-HCl / SDS system (Figure 6), one can also identify the critical pH below which an interaction was detected ($\text{pH}^{\text{crit}}(\text{EPR})$) as $\sim 7.0 \pm 0.2$. This estimate shows an excellent agreement with $\text{pH}^{\text{crit}}(\text{CMC})$. Assuming that these two estimates of pH^{crit} reflect the same facet of the onset of the interaction, the charge on the polymer at this pH equates to $-0.31 (\pm 0.02)$ *e*/monomer, corresponding to 69 (± 2) % ionization of nitrogen 2 and 100% ionization of the $-\text{COO}^-$ (H) group with negligible ionization of nitrogen 3. The fact that both the polymer and the surface are negatively charged and yet an interaction occurs suggests a significant hydrophobic contribution to the interaction.

For the ISA23-HCl /lyso-PC system, and in agreement with the surface tension experiments, the EPR studies showed no spectral changes over the pH range studied (5.5–9.0), confirming no interaction. It was interesting to note that in the absence of the ISA23-HCl, the low field peak was already significantly weaker than the center peak, indicating that the spin-probe was much more motionally constrained compared to the SDS case (Figure 5). Further, in the case of lyso-PC there is some unresolved coupling between the spin-probe and the surfactant, leading to the weak, broad resonance superimposed on the center of the spectrum. While interesting, this signal does not affect

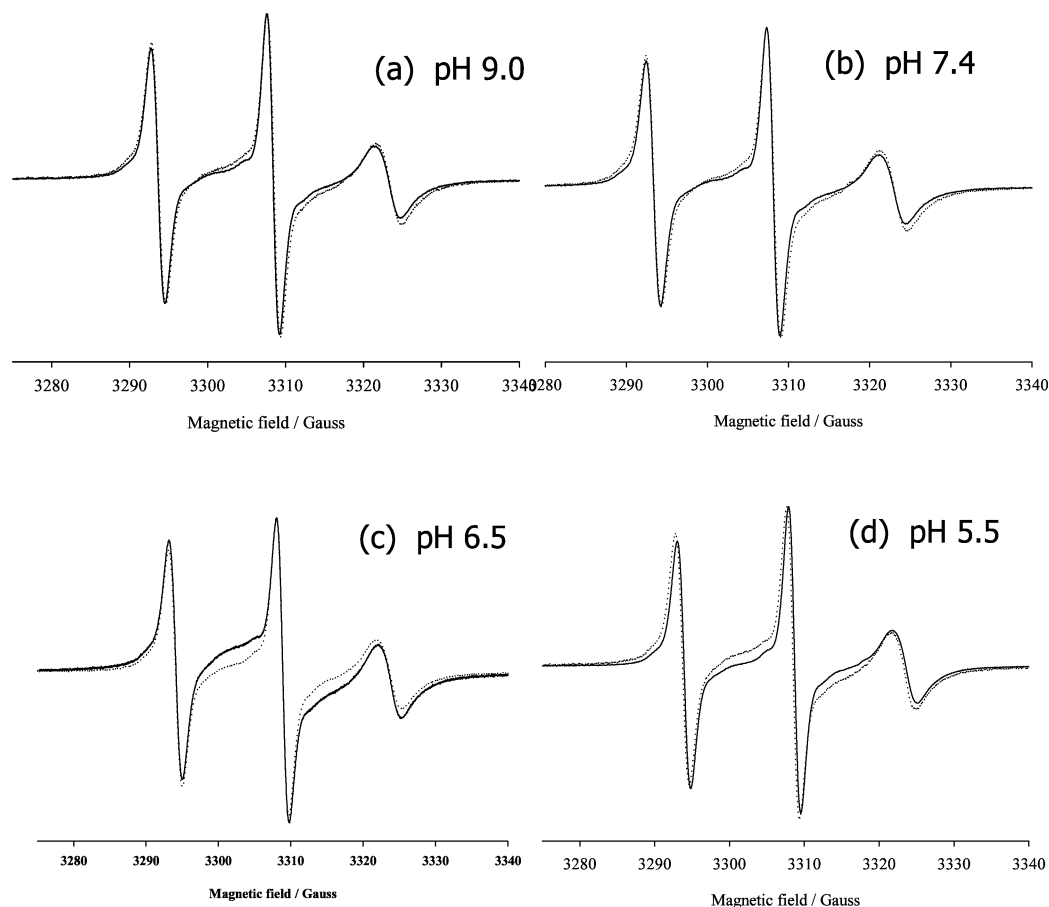


Figure 5. The effect of pH on the EPR spectrum of 16DSE solubilized in aqueous solutions of 1-palmitoyl-2-hydroxy-*sn*-glycero-3-phosphocholine (lyso-PC) in the absence (broken line) and presence (solid line) of ISA23-HCl (0.2 wt %).

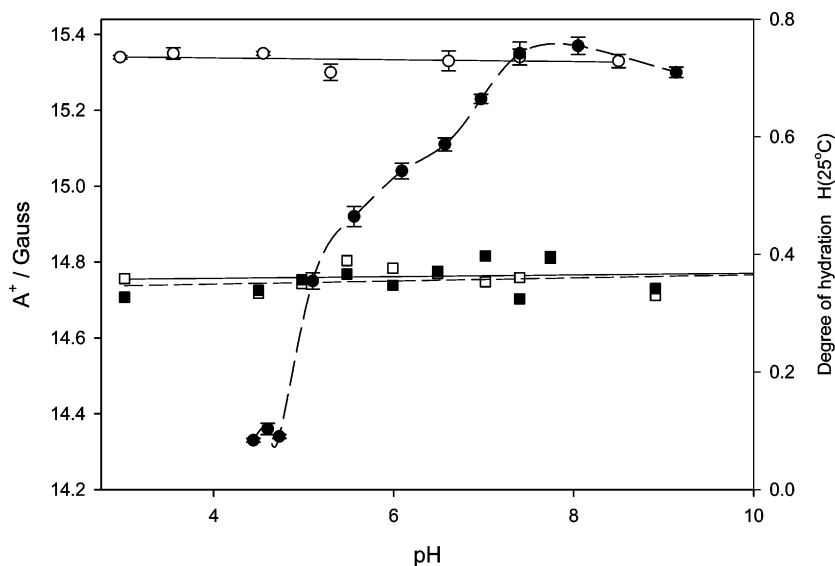


Figure 6. EPR-derived headgroup hydration of micelles formed in aqueous solution of 25 mM sodium dodecyl sulfate (SDS) (circles) or 1-palmitoyl-2-hydroxy-*sn*-glycero-3-phosphocholine (lysoPC) (squares) (at 37 °C) in the absence (open symbols) and presence (filled symbols) of ISA23-HCl (0.2 wt %) as a function of pH.

the position of the three lines arising from the spin-probe and therefore has little bearing on the data presented here.

Small-Angle Neutron Scattering. ISA23-HCl showed weak scattering at all pH values (Figure 7). When added to an SDS solution (25 mM) at pH 7.4, the ISA23-HCl /SDS scattering was virtually identical to the SDS control with the exception of a slight offset due to the background polymer scattering. However, at pH 5.5 and 4 (Figure 7b,c), the scattering was

significantly different from the control, in particular at low Q where the scattering is sensitive to larger dimensions. At pH 4 (Figure 7c), the upturn in the scattering at low Q was indicative of an attractive interaction, clearly a consequence of the same process that resulted in the phase separation observed in the surface tension data. The scattering data obtained for the ISA23-HCl /SDS mixtures at each pH were fitted using a core-shell model modified to include an element accounting for the

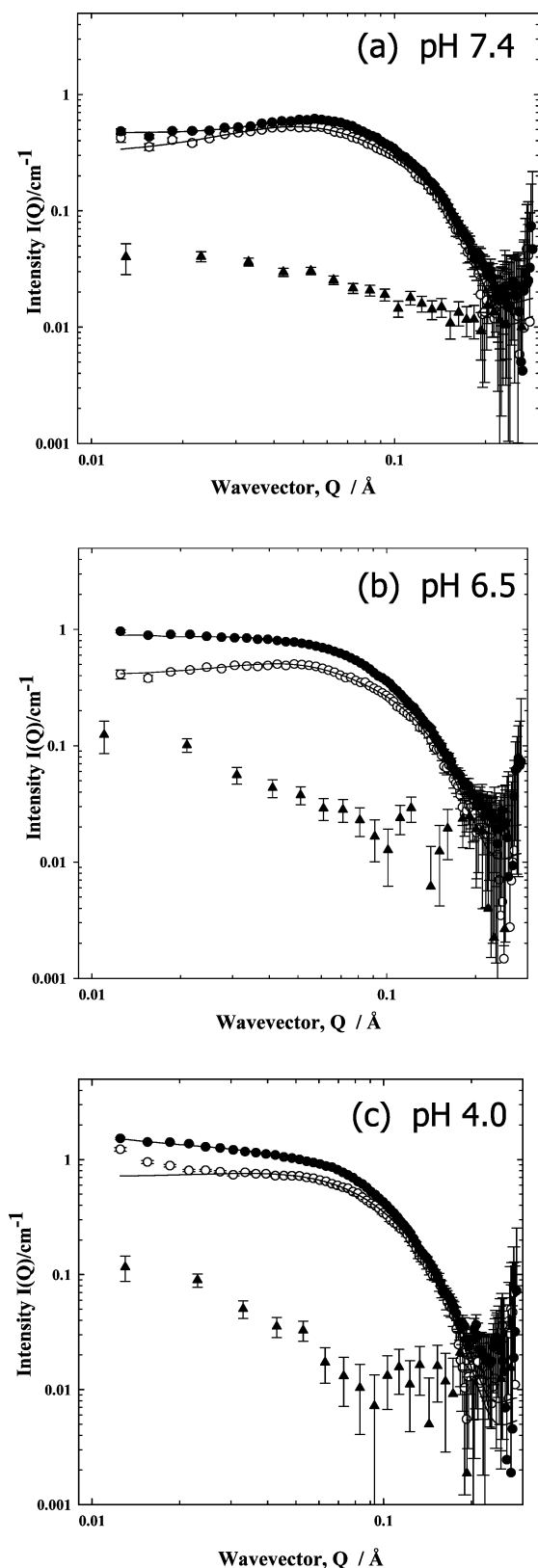


Figure 7. The effect of pH on the small-angle neutron scattering from aqueous solutions of sodium dodecyl sulfate (SDS) at a surfactant concentration of 25 mM, in the absence (open circles) and presence (filled circles) of ISA23-HCl (1.0 wt %). Also shown is the scattering from ISA23-HCl (1.0 wt %, triangles) for comparison.

polymer contribution, as described below (Table 3). One exception was the analysis of the data at pH 7.4, where there was no apparent polymer interaction (in agreement with the EPR and surface tension measurements). Here, the scattering from

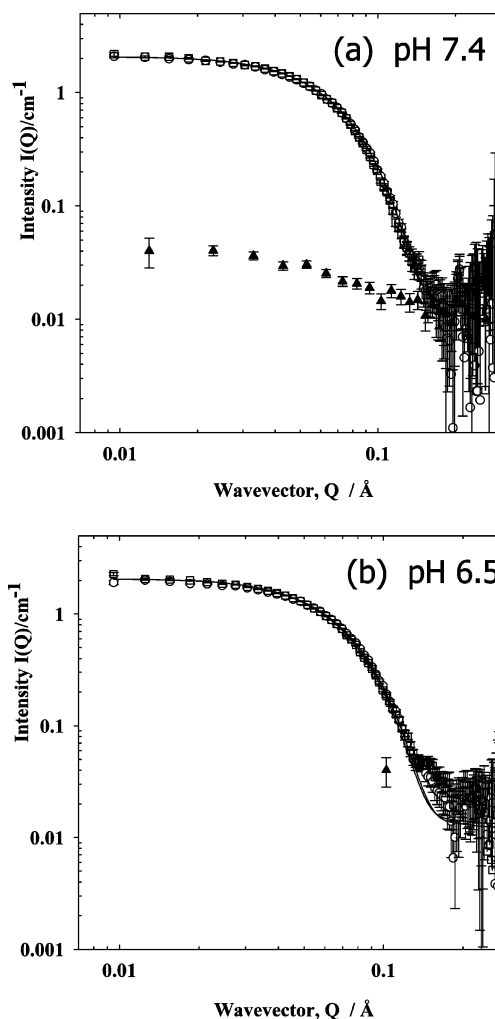


Figure 8. The effect of pH on the small-angle neutron scattering from aqueous solutions of 1-palmitoyl-2-hydroxy-*sn*-glycero-3-phosphocholine (lysoPC) at a surfactant concentration of 5 mM, in the absence (circles) and presence (squares) of ISA23-HCl (1.0 wt %). Also shown is the scattering from ISA23-HCl (1.0 wt %) for comparison.

the polymer alone was merely subtracted from that of the polymer/surfactant case during data fitting. In actual fact, this correction made a minimal difference, but the absolute intensity was marginally better reproduced. Such a simple approach for data handling was less successful for the lower pH values, undoubtedly as a consequence of polymer–surfactant interaction.

Since the EPR experiments allow estimation of the amount of water associated with the polar surface, an estimate of the amount of polymer associated within the palisade region may be obtained from the difference in $\Phi_{\text{H}_2\text{O}}$ between the experiments conducted in the presence and absence of polymer (Table 3). With the volume and approximate number of the surfactant headgroups in the micelle, and the amount of water and polymer present in the polar shell (EPR), the scattering length density and thickness of the shell were calculated (albeit using some approximations). This approach showed clearly that the micelle interacting with polymer becomes more elliptical at lower pH values (Table 3). The decreasing shell thickness was a real effect, although the value of the number may be less precise, given the assumptions made above.

To elaborate this analysis, the contribution to the overall scattering from the polymer and surfactant micelle was separated by an approach known as “contrast variation”. In essence, the deuterated micelle showed minimal scattering in deuterated water and thus any observed scattering was dominated by the

Table 3. Analysis of the SANS Scattering Data Obtained for SDS Micelles in the Presence and Absence of Polymer Using the Core–Shell Ellipse Model^a

model	pH	R_{core} (Å)*	δ_{shell}	X	$\Phi_{\text{H}_2\text{O}}^*$	N_{agg}
SDS ^b	7.4	16.7	3.2	1.3	0.65	75
	5.5	16.7	3.2	1.4	0.65	75
	4.0	16.7	3.5	1.7	0.60	95
SDS + ISA23-HCl (1 wt %)	7.4	16.7	3.2	1.4	0.65	77
	5.5	16.7	2.6	2.0	0.45	110
	4.0	16.7	2.0	2.3	0.1	120

^a R_{core} corresponds to the radius of hydrocarbon core, δ_{shell} is the thickness of the shell comprising the polar headgroups, and X is the ellipticity defined as the ratio of minor and major radii of the ellipse while $\Phi_{\text{H}_2\text{O}}$ is the degree of headgroup hydration. N_{agg} corresponds to the micelle aggregation number calculated from the volume of the hydrocarbon core of the micelle and the volume of a single C₁₂H₂₅ hydrophobic group (350 Å³). ^b The SDS concentration was 25 mM, and the additional input parameters were $\rho_{\text{core}} = -0.388 \times 10^{-6} \text{ Å}^{-2}$, $\rho_{\text{shell}} = 3.3 \times 10^{-6} \text{ Å}^{-2}$, $\rho_{\text{solv}} = 6.3 \times 10^{-6} \text{ Å}^{-2}$, $V_{\text{headgroup(dry)}}/V_{\text{core}} = 0.20$ and $\phi_{\text{scatterer}} = 0.005$. * indicates that the parameter is constrained in the fitting routine.

Table 4. Parameters Describing the Fits to the ISA23-HCl/d-SDS SANS Data

parameter	d-SDS + ISA23-HCl		
	pH 4	pH 5.5	pH 7.4
radius of the core (Å)	16.5	n/a	n/a
thickness of the shell (Å)	2.3	n/a	n/a
ellipticity (X)	2.5	n/a	n/a
radius of gyration (Å)	23.3	35.6	25.0

Table 5. Parameters Describing the Core–shell Ellipse Model Fit for ISA23-HCl/lyso-PC Data in the Presence and Absence of ISA23-HCl

parameter	lyso-PC	lyso-PC + ISA23-HCl
pH 5.5		
radius of the core (Å)	20.5	21.9
thickness of the shell (Å)	12.8	13.1
ellipticity (X)	1.6	1.6
pH 7.4		
radius of the core (Å)	20.4	21.1
thickness of the shell (Å)	12.7	13.1
ellipticity (X)	1.3	1.5

(hydrogenous) polymer. When this approach was adopted, scattering data were obtained for ISA23-HCl in the presence of deuterated SDS (d-SDS) (data not shown), and the fit parameters calculated are presented in Table 4. At pH 7.4 and 5.5, the observed scattering was best interpreted by the Gaussian coil model giving a radius of gyration not dissimilar to that observed for the polymer in the absence of the micelle, plus some residual scattering from the surfactant micelle. At pH 4, this approach to data fitting failed, and the scattering *due to the polymer* was best fitted to the surfactant model, confirming conclusions from the previous analysis that the polymer “wraps” around the micelle surface adopting the size and shape of the micelle.²⁸

The scattering obtained with lyso-PC (5 mM) micelles in the presence and absence of ISA23-HCl (1 wt %) at different pH values is shown in Figure 8, and the fit parameters are presented in Table 5. There was no significant change in micelle morphology as a function of pH or the presence of the polymer, again indicating no interaction.

Discussion

When surfactants are added to pure water, the surfactant molecules typically adsorb at the surface, and at CMC they start to form aggregates called micelles. These can have different shapes (e.g., spherical, cylindrical) that are determined by their surfactant chemistry, the “surfactant number” or the packing parameter, solvent used, pH, temperature, and type of salt

present. The number of surfactant molecules needed to form the micelle is called the “aggregation number”. This is usually high (~50–1000) and is greatly influenced by factors such as pH, temperature, ionic strength, and the nature and the purity of the surfactant. The addition of polymers to a series of surfactant solutions can have a rather complex effect on the appearance of the surface tension behavior of the resultant mixture.

The interaction between SDS and ISA23-HCl leads to a reduction in the free surfactant concentration, which drives a perturbation of the composition and structure of the species at the air–water interface, reflected in the surface tension. Changes in the surface tension therefore reflect the nature of the interaction, the strength of which increased as the pH drops. Concomitantly, the interaction leads to an elongation of the micelle, an associated increase in aggregation number, with the polymer tightly wrapped around the micelle. This behavior is rather similar to many other synthetic polymers and polyampholytic/surfactant systems.²⁹ One important feature of the highly curved surfactant micelle is the degree of hydration of the headgroups; for SDS, approximately 70% of the polar shell volume is occupied by water, and this water is in contact with the hydrocarbon core of the micelle, Figure 5. On adsorption of a polymer into this region, the contact between the water and the core is reduced, leading to favorable enthalpic and entropic contributions to the free energy of micellization. The addition of the nonionic surfactant to the ionic micelle reduced the tendency of the polymer to bind to the surface at any given pH since the bulky headgroups introduce steric hindrance across the micelle surface, and they themselves displace some water, further reducing any hydrophobic contribution arising from binding of the polymer. A full comparison of the with- and without-polymer datasets is not possible since the composition of the bound micelle and the counterion binding has not been quantified and was beyond the scope of this study, but serves to underline how subtle changes in interface composition may have a significant effect on the interaction with a polymer.

For the zwitterionic phosphocholine headgroup over this narrow pH range, a subtle balance of electrostatic interactions exist. The behavior of the phosphate group in the phosphocholine headgroup is closely analogous to the sulfate headgroup in SDS, but clearly the quaternary ammonium ion introduces an additional electrostatic term not present in SDS. Importantly, steric factors due to the much bulkier phosphocholine headgroup play a role. For the phosphocholine, the amount of displaceable water is much reduced, and thus the hydrophobic effect is greatly minimized.³⁰ Comparing the lyso-PC and SDS cases, a 50% reduction in the degree of hydration of the surfactant headgroups is sufficient to “turn off” the interaction.

Probe molecules are a powerful approach to study the local structure and dynamics of compartmentalized systems. Here, EPR spectroscopy has been used to study, *via* the hyperfine coupling constant, the degree of hydration of 16-DSE solubilized in model micelles in the presence and absence of ISA23·HCl. 16-DSE is an ideal choice of spin-probe, as its high intrinsic flexibility leads to spectra with narrow line-widths. Changes in the amount of water associated with the headgroup region gives a direct indication of the volume of polymer within the micelle palisade region while the mobility of the spin-probe provides a separate and complimentary measure of the impact of the polymer on the structure and dynamics of the micelle, as sensed by the spin-probe. A strong binding of the polymer leads to a much less fluid structure, a conclusion that has an obvious relevance to the behavior of biological membranes.

Conclusions

The interaction between the amphoteric, pH-responsive, endosomolytic polymer ISA23·HCl and model surfactant micelles was quantified and its effect on micelle dynamics studied. At pH values where the polymer and micelle bore opposite charge, electrostatic interaction resulted in micelle phase separation. However, no interaction was observed when the two species bore significant levels of the same charge. Over the pH range (7.4–5.0), that experienced during polymer trafficking through the endosomal/lysosomal system, there was an interaction between ISA23·HCl and SDS micelles even though both species carry a negative charge, suggesting a hydrophobic contribution to binding. Introduction of bulky headgroups weakened the interaction by reducing this hydrophobic contribution. Therefore, a simple electrostatic mechanism is insufficient to explain ISA23·HCl-induced membrane permeabilization and suggests that polymer chemistries with low levels of a hydrophobic comonomer able to promote greater hydrophobic interaction of a weak polyampholyte with the surface might produce endosomolytic systems of higher efficiency.^{31–33} However, when designing such polymers, care must be taken not to introduce increased nonspecific toxicity, aggregation, or reduced polymer solubility.

Acknowledgment. This work was supported by Cardiff University (Z.K.'s Ph.D. studies), and from EPSRC (GR/S25456/01), especially in the form of a Platform Grant (EP/C013220/1), and CCLRC is thanked for a provision of neutron beamtime. Dr. Damien M. Murphy is thanked for critically reading the manuscript.

References and Notes

- (1) Edelstein, M. L.; Abedi, M. R.; Wixon, J.; Edelstein, R. M. *J. Gene Med.* **2004**, *6*, 597–60.
- (2) Haccin-Bey-Abina, S.; von Kalle, C.; Schmidt, M.; Le Deist, F.; Wulfraat, N.; McIntyre, E.; Radford, I.; Villeval, J. L.; Fraser, C. C.; Cavazzana-Calvo, M.; Fischer, A. *N. Engl. J. Med.* **2003**, *348*, 255–256.
- (3) Check, E. *Nature* **2003**, *423*, 573–574.
- (4) Raper, S. E.; Chirmule, N.; Lee, F. S.; Wivel, N. A.; Bagg, A.; Gao, G. P.; Wilson, J. M.; Batshaw, M. L. *Mol. Genet. Metab.* **2003**, *80*, 148–158.
- (5) Wagner, E. *Pharm. Res.* **2004**, *21*, 8–14.
- (6) Wagner, E.; Kloeckner, J. *Adv. Polym. Sci.* **2006**, *192* (Polymer Therapeutics I), 135–173.
- (7) Putnam, D. *Nat. Mater.* **2006**, *5*, 439–451.
- (8) Ferruti, P.; Marchisio, M. A.; Duncan, R. *Macromol. Rapid Commun.* **2002**, *23*, 332–335.
- (9) Richardson, S. C. W.; Ferruti, P.; Duncan, R. *J. Drug Targeting* **1999**, *6*, 391–404.
- (10) Richardson, S. C. W.; Patrick, N. G.; Stella Man, Y. K.; Ferruti, P.; Duncan, R. *Biomacromolecules* **2001**, *2*, 1023–1028.
- (11) Patrick, N. G.; Richardson, S. C. W.; Casolaro, M.; Ferruti, P.; Duncan, R. *J. Controlled Release* **2001**, *77*, 225–232.
- (12) Wan, K. W.; Malgesini, B.; Verpilio, I.; Ferruti, P.; Griffiths, P. C.; Paul, A.; Hann, A. C.; Duncan, R. *Biomacromolecules* **2004**, *5*, 1102–1109.
- (13) Khayat, K.; Griffiths, P. C.; Grillo, I.; Heenan, R. K.; King, S. M.; Duncan, R. *Int. J. Pharm.* **2006**, *317*, 175–186.
- (14) Griffiths, P. C.; Paul, A.; Khayat, Z.; Wan, K. W.; King, S. M.; Grillo, I.; Schweins, R.; Ferruti, P.; Franchini, J.; Duncan, R. *Biomacromolecules* **2004**, *5*, 1422–1427.
- (15) Ferruti, P.; Marchisio, M. A.; Barbucci, R. *Polymer* **1985**, *26*, 1336–1348.
- (16) Griffiths, P. C.; Cheung, A. F. C.; Jenkins, R.; Pitt, A. R.; Howe, A. M.; Heenan, R. K.; King, S. M. *Langmuir* **2004**, *20*, 1161–1167.
- (17) Griffiths, P. C.; Roe, J. A.; Jenkins, R. L.; Reeve, J.; Cheung, A. Y. F.; Hall, D. G.; Pitt, A. R.; Howe, A. M. *Langmuir* **2000**, *16*, 9983–9990.
- (18) Hayter, J. B.; Penfold, J. *Colloid Polym. Sci.* **1983**, *261*, 1851.
- (19) Hayter, J. B.; Penfold, J. *Mol. Phys.* **1981**, *42*, 109.
- (20) Penfold, J.; Tucker, I.; Thomas, R. K.; Zhang, J. *Langmuir* **2005**, *21*, 10061–10073.
- (21) Bales, B. L. Inhomogeneously Broadened Spin-Label Spectra. In *Biological Magnetic Resonance*; L. J. Berliner, L. J., Reuben, J., Eds.; Plenum Publishing Corporation: New York, 1989, Vol. 8; pp 77.
- (22) Bales, B. L.; Stenland, C. *J. Phys. Chem.* **1993**, *97*, 3418.
- (23) Griffiths, P. C.; Finney, G.; Cheung, A. Y. F.; Howe, A. M.; Pitt, A. R.; King, S. M.; Heenan, R. K.; Bales, B. L. *Langmuir* **2002**, *18*, 1065–1072.
- (24) Griffiths, P. C.; Cheung, A. Y. F.; Farley, C.; Paul, A.; Heenan, R. K.; King, S. M.; Pettersson, E.; Stilbs, P.; Ranganathan, R. *J. Phys. Chem. B* **2004**, *108*, 1351–1356.
- (25) Rosen, M. J. *Surfactants and Interfacial Phenomena* 2nd Ed., Wiley-Interscience (1989), New York.
- (26) Griffiths, P. C.; Bales, B. L.; Howe, A. M.; Pitt, A. R.; Roe, J. A. *J. Phys. Chem. B* **2000**, *104*, 264–270.
- (27) Bales, B. L.; Ranganathan, R.; Griffiths, P. C. *J. Phys. Chem.* **2001**, *105*, 7465–7473.
- (28) Quina, F. H.; Nassar, P. M.; Bonilha, J. B. S.; Bales, B. L. *J. Phys. Chem.* **1995**, *99*, 17028–31.
- (29) Griffiths, P. C.; Cheung, A. Y. F.; Farley, C.; Paul, A.; Heenan, R. K.; King, S. M.; Pettersson, E.; Stilbs, P.; Ranganathan, R. *J. Phys. Chem. B* **2004**, *108*, 1351–1356.
- (30) Griffiths, P. C.; Cheung, A. Y. F.; Farley, C.; Fallis, I. A.; Howe, A. M.; Pitt, A. R.; Heenan, R. K.; King, S. M.; Grillo, I. *Langmuir* **2004**, *20*, 7313–7322.
- (31) Griffiths, P. C.; Cheung, A. Y. F. *Mater. Sci. Technol.* **2002**, *18*, 591–599.
- (32) Griffiths, P. C.; Paul, A.; Khayat, Z.; Heenan, R. K.; Ranganathan, R.; Grillo, I. *Soft Matter* **2005**, *1* (2), 152–159.
- (33) Murthy, N.; Robichaud, J. R.; Tirell, D. A.; Stayton, P. S.; Hoffman, A. S. *J. Controlled Release* **1999**, *61*, 137–143.
- (34) Yessine, M. A.; Lafleur, M.; Peterreit, H. U.; Meier, C.; Lerous, J. C. *Biochim. Biophys.* **2003**, *1613*, 28–38.
- (35) Duncan, R. *Nat. Rev. Cancer* **2006**, *6*, 688–701.

BM060930W